FRACTURE OF PIEZOELECTRIC MEMS STRUCTURES

D.F. Bahr, A.L. Olson, M.S. Kennedy, K.R. Morasch, C.D. Richards, and R.F. Richards
School of Mechanical and Materials Engineering, Washington State University, Pullman, WA 99164-2920, USA

ABSTRACT

In thin film systems subject to mechanical strains, such as those experienced in Micro Electro Mechanical Systems (MEMS), failure often occurs via fracture mechanisms. Both through thickness cracking and interfacial delamination leading to failure of the device or layer are possible failure modes. Measuring the stress at which fracture occurs in these thin film systems requires testing methods amicable to both the small scale of the films as well as the complex relationship between the mechanical properties of the film and the substrate. This paper will focus on piezoelectric oxide film systems for MEMS, a piezoelectric ceramic (PZT) on platinum. The behavior of PZT membranes at high deflections and strains for use as power generators will be examined. Experiments have been conducted with a bulge tester to obtain pressure-deflection relationships and residual stresses of the piezoelectric membranes. Comparisons are made between bulge testing to fracture with a nanoindentation method developed for testing fracture of hard coatings on soft substrates. The PZT films are fabricated by solution deposition and heat treating, which leads to significant tensile stresses in the film. The strain at failure in these PZT films, when measured with nanoindentation, is approximately 1.6 GPa, while the applied stress at failure during bulge testing is near 130 MPa. These order of magnitude differences in stresses required for failure between the bulk and the nanoscale tests will be discussed in terms of differences in flaw population as well as the effects of residual stresses. In particular, when the PZT films are first deposited as amorphous films the strength is near 3 GPa when measured via nanoindentation. The crystallization process, required to form the perovskite crystal structure leads to either a change in fracture toughness or a change in the flaw size. Based on the lowering of applied stresses required for fracture within increasing volume sampled, the flaw size is the likely controlling factor in the fracture of these MEMS structures.

1 INTRODUCTION

The need for miniaturized power sources for MEMS and microelectronics devices has long been recognized. Among the micro-scale concepts to generate electrical power are fuel cells, static heat engines and dynamic heat engines. Recent work at Washington State University has led to the development of a micro heat engine that incorporates a thin-film piezoelectric membrane generator of lead zirconate titanate ($PbZr_xTi_{1-x}O_3$, PZT) (Whalen [1]). PZT is attractive for MEMS applications due to its high piezoelectric and electromechanical coupling coefficients (Xu [2]), and is widely used in sensing and actuating MEMS applications (Polla [3]). The structure of the thin-film piezoelectric membrane generator chosen for the micro engine is a simple two-dimensional sandwich structure similar to that used for pressure transducers and ultrasonic transducers (Baborowski [4]).

Two methods of evaluating the mechanical response of this MEMS devices are nanoindentation and bulge testing. Nanoindentation can be used to measure mechanical properties of thin films. However, when thin films that are significantly harder than the underlying materials are strained, they rarely fail via mechanisms of plastic deformation. Instead, complex fracture behavior is the likely failure mechanism. As outlined by Page and Hainsworth [5], there are several possible mechanisms of failure that can be observed by examining the load – depth curve during nanoindentation, leading to their description of using this curve as a "mechanical fingerprint" of a material. Bulge testing has been used in previous studies to examine the elastic and plastic properties of thin films, as well as characterizing the residual stress in the films (Vlassak [6]). Bulge testing can also be used to pressurize membranes to failure. This provides an interesting mechanism to compare a relatively bulk fracture test (bulge testing of membranes on the order of

μm's in thickness and mm's in length) to a smaller scale nanoindentation fracture test (where μm's in thickness and lateral dimensions are probed).

2 EXPERIMENTAL PROCEDURES

The PZT film chosen for this study was $Pb(Zr_xTi_{1-x})O_3$ (PZT), where x=0.4 or 0.52. These chemistries produce films that are tetragonal (0.4) or rhombohedral (0.52) at room temperature. The films were deposited via solution deposition onto platinized silicon wafers which had been bulk micromachined to form boron doped silicon membranes which are between 1.5 and 2 μm thick. The films were deposited using a sol gel method. The samples were then pyrolized on a hot plate at approximately 375 ºC for two minutes. This process can be repeated up to three times, after which the samples were crystallized in a conventional furnace for 10 minutes at 700 ºC. After PZT processing standard photolithography can be used to pattern electrodes and the PZT film.

Two different Pt/PZT systems were used in this study. The samples for bulge testing were 1.5 μm thick Si/100 nm SiO_2/15 nm Ti/ 175 nm Pt/ 1.5 μm PZT/ 300 nm Au. The set for indentation testing were bulk silicon wafers with 100 nm SiO_2 / 20 nm Ti/ 500 nm Pt/ 180 nm PZT and were tested in both the as pyrolized and crystallize condition. The difference in thickness for the indentation test samples was to ensure the "hard film soft substrate" combination could be met.

Films were tested in a static – dynamic bulge testing system described in more detail by Hall et. al. [7]. In summary, an interferometer can be used to measure the out of plane deflection of a square membrane which is pressurized with a fluid (a gas for static testing and a liquid for dynamic testing). The laser used for interferometry can be pulsed so that deflections of the membrane can be captured at any point during cyclic testing. However, once the membrane bulges past the point at which individual fringes can be resolved, the strain cannot be directly measured. In these cases the initial pressurization of the membrane was modeled using the relationship (Bonnotte [8])

$$P(w) = \frac{c_1 \sigma_r t w}{a^2} + \frac{c_2 E t w^3}{a^4} \qquad (1)$$

where P is the applied pressure, w is the maximum deflection of the membrane, E, t, and ν are the film modulus, thickness, and Poisson's ratio, and a is half the side length of the membrane. Since this is a composite membrane, we simplify and approximate the system by using an effective modulus, based on the thickness weighted values of plane strain modulus in composite form. This model is used to determine the effective residual stress (σ_r. The constants c_1 and c_2 are 3.4 and 1.82 (Bonnotte [8]). The system is then pressurized to failure (membrane rupture), and the pressure at which failure occurs is noted, and then using the fit from eq. (1) the maximum out of plane deflection is determined. Using this deflection, the strain at the center of the membrane is given by

$$\varepsilon = C w^2 / a^2 \qquad (2)$$

where C= 0.883 at the membrane center, for a Poisson's ratio of 0.27. This calculation assumes a negligible residual stress in an energy minimization routine that minimizes the difference between strain energy and pressure energy. The maximum strain occurs on the edges of a square membrane, a distance a from the corners.

Indentations were performed using a Hysitron Triboscope with a cube corner tip that has a relatively large radius of curvature (852 nm). This means that all testing was in the portion of the tip best approximated using a spherical geometry. Indentations were carried out with fixed loading rates, using a load – hold – unload – hold – unload pattern to account for any thermal drift in the system during testing.

3 RESULTS AND DISCUSSION

Bulge testing of membranes can be carried out by pressurizing either the "front" or "back" of the membrane. Both types of experiments were carried out in this study. Figure 1 shows the geometries used for testing, and figure 2 demonstrates the difference between the failure strains when testing from these two directions. The Si-PZT membrane is stronger when pressurized from the "back" than the front, by almost a factor of two. If we examine the strain field during bulge testing, when pressurized from the front the PZT film is in bending and tension at the highest strain regions of the sample, whereas when pressurized from the back the PZT is in bending compression. Therefore, it appears that the failure in PZT / Si membranes is linked to tensile strains in the PZT film. The etched structure referred to in figure 2 refers to removing the PZT from the high strain regions, and is shown in figure 3. By etching the PZT from these regions, the strength of the membrane increased by approximately 40% when pressurized from the "front", but remains unchanged when pressurized from the "back". This further supports the model that film fracture in PZT films on silicon membranes is dominated by tensile bending in the PZT film.

A smaller scale mechanical measurement using nanoindentation testing was carried out on both amorphous and crystalline films. In both cases film fracture events can be observed during the testing, as shown in figure 4 by the small discontinuities during loading. In addition, the behavior of the underlying Pt film was determined to have a hardness of 1.65 GPa. Using the elastic modulus of the PZT film measured with the dynamic stiffness method in the Hysitron Triboscope (60 GPa for the amorphous films and 70 GPa the crystalline films) it is then possible to calculate the radial stress, σ_f at film fracture using (Pang [9])

$$\sigma_f = .357E\frac{\delta^2}{c^2} + 2.198E\frac{\delta t}{c^2} \tag{3}$$

where δ is the downward deflection of the film at the beginning of the fracture event, h is the film thickness, E the film's elastic modulus and c the plastic zone size in the underlying Pt. To estimate this value we make the simplified assumption that the maximum plastic zone size would be the total load on the indenter (a gross simplification from previous work (Pang [9]). This is required because of the relative difficulty in separating the portion of the load carried by the film's bending and stretching with this relatively thicker hard film and not an infinitely thick substrate as was the case in previous work of Pang. This leads to a film fracture stress of 1.6 GPa for the crystalline film, and 3.4 GPa for the amorphous film. Because of this assumption these values are lower bound estimates of film strength.

One other issue regarding fracture in MEMS devices is the effect of residual stresses on the fracture of these films. By altering the thickness and heat treatments of the PZT films, it is possible to alter the residual stresses. Films were fabricated and then individually bulge tested to determine the residual stress by curve fitting pressure – deflection data (figure 5) to eq. 1. The films were then bulge tested to failure to determine the applied strain at fracture. The applied maximum strain to cause failure decreased with increasing residual stress, as shown in figure 6. Note, at low residual stresses the strain at failure is approximately 1%.

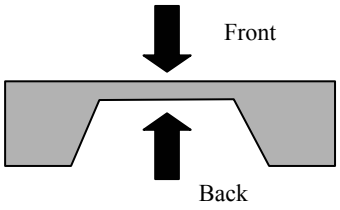

Figure 1. Schematic of pressure applied to anisotropically etched membranes.

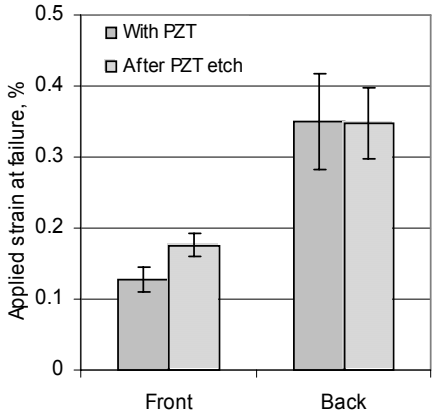

Figure 2. Applied strain to cause failure in membranes with blanket PZT layers and PZT etched from the high strain regions.

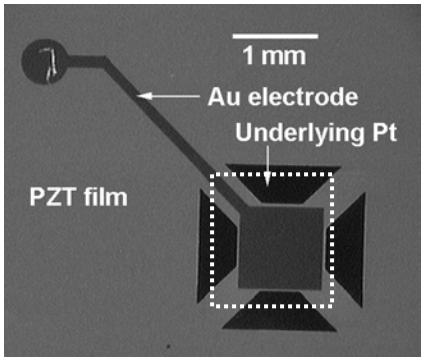

Figure 3. Optical micrograph of top of PZT membrane with PZT teched from the high strain regions of the membrane. Dotted line shows location of membrane

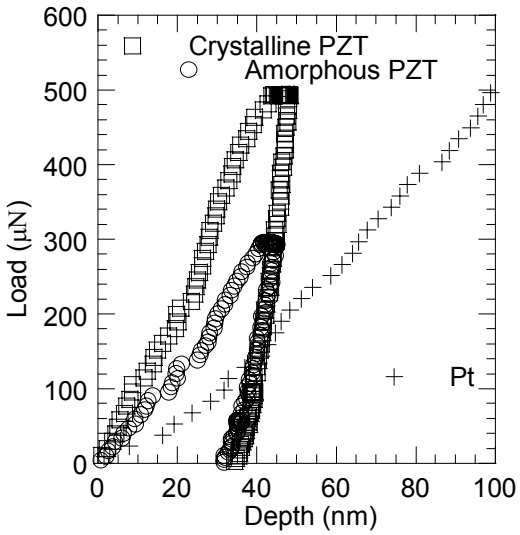

Figure 4. Nanoindentation discontinuities during loading, indicating film fracture in crystalline and amorphous PZT thin films.

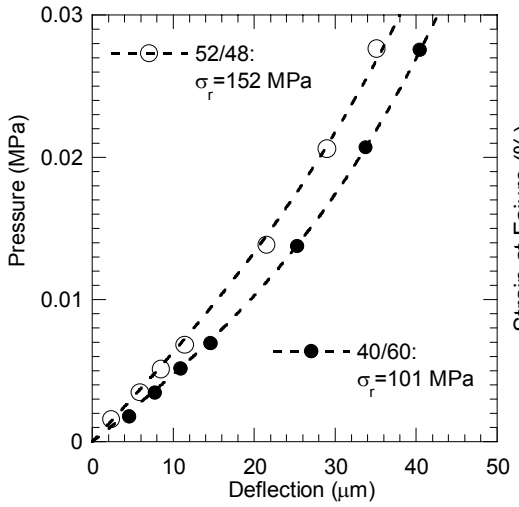

Figure 5. Pressure deflection of 52:48 and 40:60 PZT films on Si membranes. Note increased membrane σ_r with the 52:48 film.

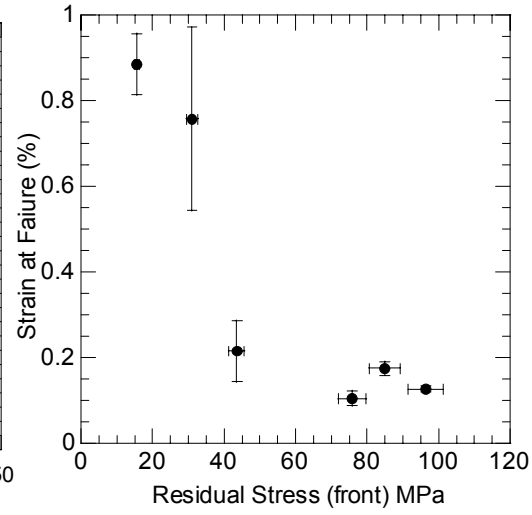

Figure 6. Reduction in the strain at failure with increased residual stress.

To compare to first order the difference in bulge testing and the indentation stress, the applied strain at failure in the PZT can be converted to a tensile stress by multiplication of the biaxial modulus. This leads to an applied stress at failure of 130 MPa for the bulge test of the 1 μm thick PZT film, and a 1.6 GPa stress at failure for the 180 nm thick PZT film. This order of magnitude discrepancy may be due to the difference in the volume of PZT samples in each method. In the case of the bulge testing, lateral regions of mm's of PZT are strained, whereas in the indentation testing the lateral areas tested are on the order of 1-2 μm^2 . This suggests that the flaw density is extremely broad, and by sampling larger volumes statistically a larger flaw will be found in the bulge test. One other possibility is that that the residual stress in the films generated for nanoindentation are significantly less than the stresses in the PZT films used for bulge testing. This could be due to either the thicker platinum film used in the nanoindentation tests which will lead to differences in thermal expansion during cooling, or the difference in thickness of the PZT film itself. If we make the assumption that the films fabricated for indentation have a low tensile stress (say 10 MPa), then the corresponding applied tensile strain to failure in the bulge testing system would be almost 1%. With a modulus of approximately 70 GPa, a 1% applied strain would be 700 MPa. This is significantly closer (within a factor of two) to the results from the nanoindentation fracture tests, and is a possible explanation for this discrepancy. If the PZT film system measured via nanoindentation has a lower residual stress as well as having sampling a smaller volume, then the nanoindentation results should indeed be larger than the bulge test results.

4 SUMMARY

The fracture of piezoelectric oxide films on compliant substrates has been examined using a small scale nanoindentation test and a more macroscopic bulge testing method. Bulge testing shows

film fracture occurs during the point of largest applied tensile stresses to the oxide films. Indentation testing to fracture in PZT films suggests that the crystallization process in which the amorphous film is heat treated to develop the piezoelectric phases weakens the film (from applied tensile stresses at fracture of 3.4 to 1.6 GPa). Bulge testing results exhibit fracture at an order of magnitude lower applied stresses. If the thicker platinum and thinner PZT layers lead to lower residual stresses, then the nanoindentation results are about a factor of two higher than the bulge test results. This suggests the differences are caused by both the residual stress differences between the two systems and the flaw density sampled by the two tests since the bulge tests samples lengths of mm's, while the indentation tests sample lengths of μm's.

5 ACKNOWLEDGMENTS

The authors would like to thank Dr. N.R. Moody of Sandia National Laboratories for helpful discussions, and acknowledge the financial support of the U.S. DARPA MTO's MicroPower Generation Program and the U.S. Army SMDC contract #DASG60-02-C0001.Department of Energy. Additional financial support was provided by through the U.S. Department of Energy PECASE program under contract DE-AC04-94AL85000

6 REFERENCES

1. Whalen S., Thompson M., Bahr D., Richards C., and Richards R., "Design, Fabrication and Testing of the P3 Micro Heat Engine", Sensors and Actuators, A104, 200-208 (2003).
2. Xu R., Trolier-McKinstry S., Ren W., Xu B., Xie Z.-L., Hemker K.J., "Domain wall motion and its contribution to the dielectric and piezoelectric properties of lead zirconate titanate films", Journal of Applied Physics. 89, 1336-1348 (2001).
3. Polla D.L., Francis L.F., "Processing And Characterization Of Piezoelectric Materials And Integration Into Microelectromechanical Systems", Annual Review of Materials Science, 28, 563-597 (1998).
4. Baborowski J., Ledermann N., Muralt P., "Piezoelectric Micromachined Ultrasonic Transducers based on PZT Films", in Materials Research Society Symposium Proceedings, Nano- and Microelectromechanical Systems (NEMS and MEMS) and Molecular Machines eds. D. A. LaVan, A. A. Ayon, T. E. Buchheit, M. J. Madou, 741, J12.4.1-6 (2003).
5. Page T.F. and Hainsworth S.V. Using nanoindentation techniques for the characterization of coated systems: a critique", Surface and Coating Technology, 61, 201-208 (1993).
6. Vlassak J.J., Nix W.D. "A New Bulge Test Technique for the Determination of Young's Modulus and Poisson's Ratio of Thin Films", Journal of Materials Research, 7, 3242-3249 (1992).
7. Hall J.D., Apperson N.E., Crozier B.T., Xu C., Richards R.F., Bahr D.F., and Richards C.D., "A Facility for Characterizing the Dynamic Mechanical Behavior of Thin Membranes for MEMS Devices", Review of Scientific Instrumentation, 73, 2067-2072 (2002)
8. Bonnotte E, Delobelle P, Bornier L "Two Interferometric Methods for the Mechanical Characterization of Thin Films by Bulge Testing: Application to Single Crystal of Silicon", Journal of Materials Research. 12, 2234-2248 (1997).
9. Pang M. and Bahr D.F., "Thin Film Fracture During Nanoindentation Of A Titanium Oxide Film – Titanium System", Journal of Materials Reseach, 16, 2634-2643 (2001).